Eur. Phys. J. C 36, 471–482 (2004)
Digital Object Identifier (DOI) 10.1140/epjc/s2004-01974-2

THE EUROPEAN PHYSICAL JOURNAL C

Laurent series expansion of sunrise-type diagrams using configuration space techniques*

S. Groote[1,2], J.G. Körner[1], A.A. Pivovarov[1,3]

[1] Institut für Physik, Johannes-Gutenberg-Universität, Staudinger Weg 7, 55099 Mainz, Germany
[2] Füüsika-Keemiateaduskond, Tartu Ülikool, Tähe 4, 51010 Tartu, Estonia
[3] Institute for Nuclear Research of the Russian Academy of Sciences, Moscow 117312, Russia

Received: 9 April 2004 / Revised version: 28 June 2004 /
Published online: 23 July 2004 –

Abstract. We show that configuration space techniques can be used to efficiently calculate the complete Laurent series ε-expansion of sunrise-type diagrams to any loop order in D-dimensional space-time for any external momentum and for arbitrary mass configurations. For negative powers of ε the results are obtained in analytical form. For positive powers of ε including the finite ε^0 contribution the result is obtained numerically in terms of low-dimensional integrals. We present general features of the calculation and provide exemplary results up to five-loop order which are compared to available results in the literature.

1 Introduction

The computation of multi-dimensional integrals corresponding to multi-loop Feynman diagrams is a necessity for high precision calculation in quantum field theory since perturbation theory remains the main tool of most theoretical analysis' within the standard model and beyond [1–4]. An important ingredient of the algebraic approach to the evaluation of Feynman diagrams is the integration-by-parts technique which allows one to derive and analyze recurrence relations for the sets of relevant multi-loop integrals [5]. Using the integration-by-parts technique, many diagrams are reduced to simplified subsets of master integrals (see e.g. [6–14]).

An important subset of master integrals is represented by diagrams of the sunrise topology, the so-called sunrise-type diagrams (also called sunset-type, water-melon, basketball, or banana diagrams) [15–17]. Diagrams of the sunrise topology have been studied quite intensively in the past and many of their properties have been known for quite some time [6,18,19,13,20]. Physical applications are also numerously worked out in e.g. [21–25]. This concerns in particular finite temperature calculations using effective potentials [26–30]. There are also applications in nuclear and solid state physics where methods of quantum field theory are used for the construction of low-energy effective theories [31]. The importance of the sunrise topology in physical applications alone justifies the strong interest in sunrise-type diagrams [32–39]. At the same time this topology is a good laboratory for checking the efficiency of new methods of multi-loop calculations [40–42]. The relevant master integrals should be calculated as precisely as possible within dimensional regularization, the results of which should be expressed in terms of the complete Laurent series expansion in the dimensional parameter $\varepsilon = (D-4)/2$ including also positive powers of ε [43]. Higher order terms in the ε expansion are needed if the sunrise-type diagram is inserted into a divergent diagram or when one is using the integration-by-parts recurrence relation which can generate inverse powers of ε. For example, recently the Laurent series expansion for four-loop master integrals has been found using numerical methods [44]. The numerical evaluation of Feynman diagrams has become a valuable tool in higher order loop calculations because the extreme complexity of these calculations often precludes an analytical approach and thus the numerical approach is the only possibility to obtain physical results [45].

In this paper we develop and describe a configuration space method which allows one to efficiently evaluate the coefficients of the Laurent series expansion in the dimensional parameter ε for sunrise-type diagrams [46]. The method is simple to use and it works well for arbitrary mass configurations, arbitrary values of the external momentum and any number of loops.

In configuration space, the correlator function described by a sunrise-type diagram with $(n+1)$ lines (corresponding to n loops, cf. Fig. 1) is given by the product of propagators $D(x,m)$,

$$\Pi_n(x) = \prod_{i=1}^{n+1} D(x,m_i) \tag{1}$$

* Partially supported by RFBR grants # 02-01-601, 03-02-17177.

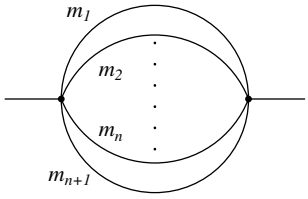

Fig. 1. n-loop diagram with $(n+1)$ lines of the sunrise-type topology

and/or their derivatives if necessary (for details see [46–48]). The propagator $D(x,m)$ of a massive particle with the mass parameter m in D-dimensional (Euclidean) space-time is given by the momentum space integral which can be evaluated in terms of Bessel functions,

$$D(x,m) = \frac{1}{(2\pi)^D} \int \frac{\mathrm{e}^{-\mathrm{i}(p\cdot x)}\mathrm{d}^D p}{p^2+m^2} = \frac{(mx)^\lambda K_\lambda(mx)}{(2\pi)^{\lambda+1}x^{2\lambda}}, \quad (2)$$

where we write $D = 2\lambda + 2$. Here $K_\lambda(z)$ is a modified Bessel function of the second kind (see e.g. [49]). In the zero mass case the propagator simplifies to $D(x,0) = \Gamma(\lambda)/4\pi^{\lambda+1}x^{2\lambda}$. It is obvious that the correlator function $\Pi(x)$ in configuration space contains no integration at all. In this respect it is a kind of analogue to a tree diagram in momentum space. A calculation of a sunrise-type diagram is necessary only if one wants to calculate the diagram in momentum space. This requires a Fourier transformation,

$$\tilde{\Pi}_n(p) = \int \Pi_n(x)\mathrm{e}^{\mathrm{i}(p\cdot x)}\mathrm{d}^D x. \quad (3)$$

Note that the required integrals are basically scalar which makes the angular integration in (3) simple in D-dimensional space-time. One obtains one-dimensional integrals

$$\tilde{\Pi}_n(p) = 2\pi^{\lambda+1} \int_0^\infty \left(\frac{px}{2}\right)^{-\lambda} J_\lambda(px)\Pi_n(x)x^{2\lambda+1}\mathrm{d}x, \quad (4)$$

where $p = |p|$ and $x = |x|$ are the absolute values of p^μ and x^μ, respecticely, and $J_\lambda(z)$ is the Bessel function of the first kind. For integrals with additional tensor structure the plane wave function $\mathrm{e}^{\mathrm{i}(p\cdot x)}$ occurring in the Fourier integral in (3) has to be expanded in a series of Gegenbauer polynomials $C_j^\lambda(w)$ [50,51]. Because this expansion does not change the principal structure of the expressions, the representation given by (4) is quite universal and will be used in the following.

This paper is organized as follows. In Sect. 2 we explain the treatment of the singular part of the integral while the calculation of the non-singular part is dealt with in Sect. 3. After a striking but quite simple example we present four- and five-loop calculations of the bubble diagram in Sect. 4. Finally, in Sect. 5 we give recipes to treat so-called irreducible numerator factors in sunrise diagrams. In Sect. 6 we present our conclusions.

2 ε-expansion of the singular part

The ultraviolet (UV) singularities that appear in the correlator function $\tilde{\Pi}(p)$ are related to the small x behavior of the integrand in (4). These singularities can be subtracted using the standard R-operation [52]. The simplest way to do this is to expand the relevant Bessel functions at small x and then to integrate the resulting integrand in $D = 4-2\varepsilon$ dimensions. However, in order to avoid infrared singularities coming from the large x-region of integration, some parts of the unexpanded Bessel functions should be retained. From a technical point of view one or two Bessel functions in the integrands can be kept unexpanded to provide the necessary cutoff. This is possible because the integrals containing one or two Bessel functions in the integrand can be done analytically. Indeed, for any μ, ν one has [53,54]

$$\begin{aligned}
&\int_0^\infty x^{\mu-1}K_\nu(mx)\mathrm{d}x = \frac{2^{\mu-2}}{m^\mu}\Gamma\left(\frac{\mu+\nu}{2}\right)\Gamma\left(\frac{\mu-\nu}{2}\right),\\
&\int_0^\infty x^{\mu-1}K_\nu(mx)K_\nu(mx)\mathrm{d}x\\
&= \frac{2^{\mu-3}}{m^\mu\Gamma(\mu)}\Gamma\left(\frac{\mu}{2}+\nu\right)\Gamma\left(\frac{\mu}{2}\right)\Gamma\left(\frac{\mu}{2}\right)\Gamma\left(\frac{\mu}{2}-\nu\right). \quad (5)
\end{aligned}$$

However, because one or two of the Bessel functions are kept unexpanded, this method breaks the natural symmetry between the masses of different lines. An alternative recipe is to introduce a damping factor into the integrand with an adequate power of n such as e.g.

$$\begin{aligned}
h(x) &= \mathrm{e}^{-\mu^2x^2}\sum_{k=0}^{n}\frac{(\mu x)^{2k}}{k!}\\
&= \mathrm{e}^{-\mu^2x^2}\left\{1+\mu^2x^2+\frac{1}{2}\mu^4x^4+\frac{1}{6}\mu^6x^6+\ldots\right\}. \quad (6)
\end{aligned}$$

One then expands all massive propagators for small x keeping only the singular terms of the integrand. For the extraction of the UV poles this is the most convenient way to proceed. At small x the damping factor behaves as $h(x) = 1 + O(x^{2n})$ which does not change the structure of the singularities of the integrand at small x if n is sufficiently large (depending on the number of lines and the dimension of space-time). Still another possibility is to use a hard cutoff in configuration space by introducing a cutoff in the integration at some given x_0 and to extract the poles from the integral over the finite interval (see e.g. [55]). Which of the three methods is the most suitable depends on the problem at hand. We found that the damping factor method is most convenient for the calculation of the pole parts. In the equal mass case it is advantageous to use the Bessel function method for the calculation of the non-singular parts of the ε-expansions since one generates more compact expressions for the necessary subsequent numerical evaluation.

When one performs a series expansion of the integrand near the origin, one easily obtains the singular parts for any sunrise-type diagram for any mass configuration. As

an example we consider the genuine two-loop sunrise diagram with three different loop masses,

$$\Pi_2(x) = D(x,m_1)D(x,m_2)D(x,m_3) \tag{7}$$

for $D = 4 - 2\varepsilon$ space-time dimensions (the index "2" in $\Pi_2(x)$ stands for the two-loop case). In this case one needs two UV counterterms for the renormalization of the divergent integral,

$$\Pi_2^{\rm ren}(x) = \Pi_2^{\rm reg}(x) - C_0\delta(x) - C_2\partial^2\delta(x), \tag{8}$$

with $\partial^2 = \partial^\mu\partial_\mu$ which will lead to a factor $-p^2$ in momentum space. The counterterms read

$$\begin{aligned} C_0 &= \mathcal{N}_2 \int \Pi_2(x) \mathrm{d}^D x \\ &= \mathcal{N}_2 \int D(x,m_1)D(x,m_2)D(x,m_3)\mathrm{d}^D x, \\ C_2 &= \frac{\mathcal{N}_2}{2D} \int \Pi_2(x) x^2 \mathrm{d}^D x \\ &= \frac{\mathcal{N}_2}{2D} \int D(x,m_1)D(x,m_2)D(x,m_3) x^2 \mathrm{d}^D x. \end{aligned} \tag{9}$$

It is clear that the program of UV renormalization requires the calculation of vacuum bubble diagrams.

Note that we use a special normalization convention for the integration measure. This is the usual integration measure for massive vacuum integrals that considerably simplifies the expressions for the counterterms (pole parts) by removing some awkward terms containing the Euler constant γ or π^2. The normalization factor is given by

$$\mathcal{N}_n = \left(\frac{(4\pi)^{2-\varepsilon}}{\Gamma(1+\varepsilon)}\right)^n \tag{10}$$

for the n-loop (or $(n+1)$-line) sunrise-type diagram.

Starting with the singular pieces for the genuine two-loop sunrise diagram with equal masses m, we obtain

$$\begin{aligned} C_0 &= m^2\left\{-\frac{3}{2\varepsilon^2} - \frac{9}{2\varepsilon}\right\} + O(\varepsilon^0), \\ C_2 &= \frac{1}{\varepsilon} + O(\varepsilon^0), \end{aligned} \tag{11}$$

where the renormalization scale μ is set to $\mu = m$. After the counterterms have been determined, external lines carrying external momenta can be added because the pole parts of the vacuum bubbles and the sunrise-type diagrams are identical. The generalization of this example to n-loop sunrise-type diagrams with any mass configuration is straightforward. In the main text we list a few sample results for equal masses, again setting the renormalization scale μ to $\mu = m$. This includes sunrise-type diagrams with vanishing outer momenta called bubble diagrams. We compute the four-loop bubble diagram also calculated by Laporta [44] whose result we reproduce. In the sample results below the normalization factor $\mathcal{N}_n$ is included according to the number of lines/loops that makes the definition of $\tilde{\Pi}_2(p^2)$ a bit different from that used in (3) and (4). The sample results are

$$\begin{aligned} \tilde{\Pi}_1(p^2) &= \frac{1}{\varepsilon} + O(\varepsilon^0), \\ \tilde{\Pi}_2(p^2) &= m^2\left\{-\frac{3}{2\varepsilon^2} - \frac{9}{2\varepsilon}\right\} - \frac{p^2}{4\varepsilon} + O(\varepsilon^0), \\ \tilde{\Pi}_3(p^2=0) &= m^4\left\{\frac{2}{\varepsilon^3} + \frac{23}{3\varepsilon^2} + \frac{35}{2\varepsilon}\right\} + O(\varepsilon^0), \\ \tilde{\Pi}_3(p^2=-m^2) &= m^4\left\{\frac{2}{\varepsilon^3} + \frac{22}{3\varepsilon^2} + \frac{577}{36\varepsilon}\right\} + O(\varepsilon^0), \\ \tilde{\Pi}_4(p^2=0) &= m^6\left\{-\frac{5}{2\varepsilon^4} - \frac{35}{3\varepsilon^3} - \frac{4565}{144\varepsilon^2} - \frac{58345}{864\varepsilon}\right\} \\ &\quad + O(\varepsilon^0), \\ \tilde{\Pi}_4(p^2=-m^2) & \\ &= m^6\left\{-\frac{5}{2\varepsilon^4} - \frac{45}{4\varepsilon^3} - \frac{4255}{144\varepsilon^2} - \frac{106147}{1728\varepsilon}\right\} + O(\varepsilon^0), \\ \tilde{\Pi}_5(p^2=0) & \\ &= m^8\left\{\frac{3}{\varepsilon^5} + \frac{33}{2\varepsilon^4} + \frac{1247}{24\varepsilon^3} + \frac{180967}{1440\varepsilon^2} + \frac{898517}{3456\varepsilon}\right\} \\ &\quad + O(\varepsilon^0), \\ \tilde{\Pi}_5(p^2=-m^2) & \\ &= m^8\left\{\frac{3}{\varepsilon^5} + \frac{16}{\varepsilon^4} + \frac{49}{\varepsilon^3} + \frac{6967}{60\varepsilon^2} + \frac{1706063}{7200\varepsilon}\right\} + O(\varepsilon^0), \\ \tilde{\Pi}_6(p^2=0) & \\ &= m^{10}\left\{-\frac{7}{2\varepsilon^6} - \frac{133}{6\varepsilon^5} - \frac{238}{3\varepsilon^4} - \frac{77329}{360\varepsilon^3} - \frac{21221921}{43200\varepsilon^2}\right. \\ &\quad \left. - \frac{2596372387}{2592000\varepsilon}\right\} + O(\varepsilon^0). \end{aligned} \tag{12}$$

Note the dependence on the external momentum p^2. This dependence has its origin in the derivatives appearing e.g. in (8). The coefficient of the leading singularity in ε is independent of p^2. In Appendix A we list results for unequal mass configurations up to four-loop order. When setting all masses equal the results of the general mass case can be seen to agree with the above equal mass results.

After having determined the singular parts of the Laurent series expansion using the damping factor method, what remains to be done is to calculate the coefficients of the positive powers of ε in the ε-expansion including the finite ε^0 term. In order to determine the non-singular parts one needs to resort to the Bessel function method. What is technically needed is to develop a procedure for the ε-expansion of Bessel functions. This will be the subject of the next section.

Starting with the next section we discuss only bubble diagrams which have a simpler structure and allow for a comparison with results in the literature (e.g. with [44]). It is clear that non-singular parts can also be calculated for sunrise-type diagrams with $p^2 \neq 0$ with our methods. For $p^2 > \sum_i m_i^2$ the calculation gives rise to absorptive parts represented by the spectral density (cf. [46,47,56]) which will not be discussed any further in this paper.

3 ε-expansion of the non-singular part

The non-singular parts in the ε-expansion of sunrise-type diagrams can also easily be calculated with the help of configuration space techniques. However, in contrast to the singular coefficients calculated in the last section, in the general case the computation of the non-singular coefficients requires a numerical evaluation. A technical problem which appears in the computation of higher order terms of the ε-expansion is the necessity to expand the Bessel functions in their indices. For the first order in ε the relevant corrections are known and can again be re-expressed in terms of Bessel functions. Using [54]

$$\left[\frac{\partial K_\nu(z)}{\partial \nu}\right]_{\nu=\pm n} = \pm\frac{1}{2}n!\sum_{k=0}^{n-1}\left(\frac{z}{2}\right)^{k-n}\frac{K_k(z)}{k!(n-k)}, \quad n\in\{0,1,\dots\} \tag{13}$$

for the derivative of the Bessel function $K_\nu(z)$ with respect to its index near integer values of this index, we obtain the series expansion

$$\begin{aligned} K_{-\varepsilon}(x) &= K_0(x) + O(\varepsilon^2),\\ K_{1-\varepsilon}(x) &= K_1(x) - \frac{\varepsilon}{x}K_0(x) + O(\varepsilon^2),\\ K_{2-\varepsilon}(x) &= K_2(x) - \frac{2\varepsilon}{x}K_1(x) - \frac{2\varepsilon}{x^2}K_0(x) + O(\varepsilon^2) \end{aligned} \tag{14}$$

for the first few Bessel functions with non-integer indices (for details cf. [56]). Note that the first two results suffice to find the expansion for the Bessel function with any integer index due to the recurrence relations that connect three Bessel functions with consecutive indices. To the best of our knowledge one has to proceed numerically for the higher order terms. At least we were not able to find a general procedure for the analytical evaluation of the finite parts of the ε-expansion. Some analytical results can be found in [57,58].

A convenient starting point for the ε-expansion is the integral representation

$$K_\nu(z) = \int_0^\infty \mathrm{e}^{-z\cosh t}\cosh(\nu t)\mathrm{d}t. \tag{15}$$

Then the expansion for $K_{-\varepsilon}(z)$ reads

$$\begin{aligned} K_{-\varepsilon}(z) &= \int_0^\infty \mathrm{e}^{-z\cosh t}\cosh(-\varepsilon t)\mathrm{d}t\\ &= \sum_{n=0}^\infty \frac{\varepsilon^{2n}}{(2n)!}f_{2n}(z), \end{aligned} \tag{16}$$

where

$$f_k(z) = \int_0^\infty t^k \mathrm{e}^{-z\cosh t}\mathrm{d}t. \tag{17}$$

The family of functions $f_k(z)$ is rather close to the original set of Bessel functions $K_\nu(z)$ and can easily be studied both analytically and numerically. The limits at $z\to 0$ and $z\to\infty$ are known analytically and are simple. They allow for an efficient interpolation for intermediate values of the argument.

For the expansion of the second basic function $K_{1-\varepsilon}(z)$ we write

$$\begin{aligned} K_{1-\varepsilon}(z) &= \int_0^\infty \mathrm{e}^{-z\cosh t}\cosh(t-\varepsilon t)\mathrm{d}t\\ &= \sum_{n=0}^\infty \frac{\varepsilon^{2n}}{(2n)!}a_{2n}(z) - \sum_{n=0}^\infty \frac{\varepsilon^{2n+1}}{(2n+1)!}b_{2n+1}(z), \end{aligned} \tag{18}$$

with

$$\begin{aligned} a_k(z) &= \int_0^\infty t^k \mathrm{e}^{-z\cosh t}\cosh t\,\mathrm{d}t,\\ b_k(z) &= \int_0^\infty t^k \mathrm{e}^{-z\cosh t}\sinh t\,\mathrm{d}t. \end{aligned} \tag{19}$$

Integration by parts and parameter derivatives can be used to further reduce integrals containing any power of the hyperbolic functions $\sinh(t)$ and $\cosh(t)$ in $f_k(z)$. The functions $f_k(z)$ allow one to calculate the higher order coefficients in the ε-expansion. Therefore, the two functions $a_k(z)$ and $b_k(z)$ are again related to the functions $f_k(z)$,

$$a_k(z) = -\frac{\mathrm{d}}{\mathrm{d}z}f_k(z), \qquad b_k(z) = \frac{k}{z}f_{k-1}(z). \tag{20}$$

Using these relations, we obtain

$$K_{1-\varepsilon}(z) = -\sum_{n=0}^\infty \frac{\varepsilon^{2n}}{(2n)!}\left(\frac{\mathrm{d}}{\mathrm{d}z}+\frac{\varepsilon}{z}\right)f_{2n}(z). \tag{21}$$

Due to recurrence relations in the index ν for the family $K_\nu(z)$ these two formulas suffice to calculate the Bessel function $K_\nu(z)$ for any ν.

The functions $f_k(z)$ satisfy the differential equation

$$\left(\frac{\mathrm{d}^2}{\mathrm{d}z^2}+\frac{1}{z}\frac{\mathrm{d}}{\mathrm{d}z}-1\right)f_k(z) = \frac{k(k-1)}{z^2}f_{k-2}(z), \tag{22}$$

related to the Bessel differential equation. The small z behavior

$$f_k(z) = \frac{1}{k+1}\ln^{k+1}\left(\frac{1}{z}\right)\left(1+O\left(\frac{1}{\ln(z)}\right)\right) \tag{23}$$

can be found by using yet another representation for the function $f_k(z)$, obtained from (17) by the substitution $u=\cosh t$,

$$f_k(z) = \int_1^\infty \frac{\mathrm{e}^{-zu}}{\sqrt{u^2-1}}\ln^k(u+\sqrt{u^2-1})\mathrm{d}u, \tag{24}$$

or directly from the behavior of the function $K_\nu(x)$ at small x,

$$K_{-\varepsilon}(x) = \frac{1}{\varepsilon}\sinh\left(\varepsilon\ln(1/x)\right). \tag{25}$$

In Fig. 2 the functions $f_n(z)$ are compared with $K_0(z)$ for various values of n. Note that $f_0(z)=K_0(z)$ and $a_0(z) = -f_0'(z) = K_1(z)$. All curves are very smooth and their

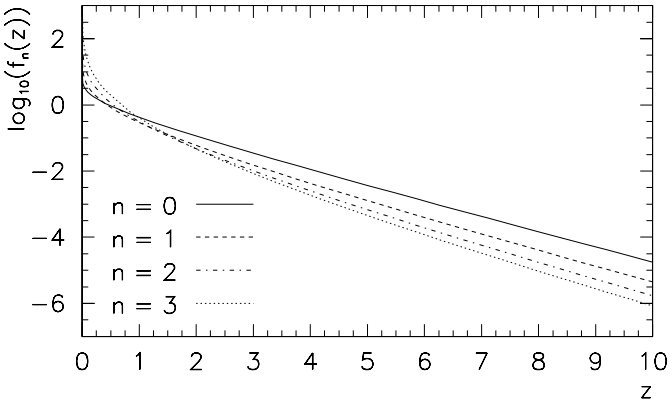

Fig. 2. Comparison of functions $f_n(z)$ for different values of n, plotted on a logarithmic scale

functional behavior is similar to that of the original Bessel function.

While in four-dimensional space-time the massive propagator contains the Bessel function $K_{1-\varepsilon}(z)$, for $D = 2$ dimensional space-time the basic function is the Bessel function $K_{-\varepsilon}(z)$, since the propagator reads

$$D(x,m)|_{D=2} = \frac{1}{2\pi} K_0(mx). \tag{26}$$

As an example for the numerical calculation of the ε-expansion using Bessel functions we consider a toy model integral related to the one-loop case in two dimensions. We select this example because the integral is finite and analytically known, so that we can compare our numerical calculation with the exact answer. Using (5), we obtain

$$2\int K_{-\varepsilon}(x) K_{-\varepsilon}(x) x \,\mathrm{d}x = \Gamma(1+\varepsilon)\Gamma(1-\varepsilon). \tag{27}$$

The expansion in ε is given by

$$\begin{aligned}\Gamma(1-\varepsilon)\Gamma(1+\varepsilon) &= \frac{\pi\varepsilon}{\sin(\pi\varepsilon)} \\ &= 1 + \frac{\pi^2\varepsilon^2}{6} + \frac{7\pi^4\varepsilon^4}{360} + O(\varepsilon^6).\end{aligned} \tag{28}$$

On the other hand, we can use the expansion

$$K_{-\varepsilon}(x) = f_0(x) + \frac{\varepsilon^2}{2} f_2(x) + \frac{\varepsilon^4}{24} f_4(x) \tag{29}$$

to rewrite the integral in the form

$$\begin{aligned}&2\int_0^\infty K_{-\varepsilon}(x) K_{-\varepsilon}(x) x \,\mathrm{d}x \\ &= 2\int_0^\infty f_0(x)^2 x \,\mathrm{d}x + 2\varepsilon^2 \int_0^\infty f_0(x) f_2(x) x \,\mathrm{d}x \\ &\quad + \frac{\varepsilon^4}{6}\int_0^\infty f_0(x) f_4(x) x \,\mathrm{d}x + \frac{\varepsilon^4}{2}\int_0^\infty f_2(x)^2 x \,\mathrm{d}x \\ &\quad + O(\varepsilon^6).\end{aligned} \tag{30}$$

Using the explicit expressions for the functions f_k we checked by numerical integration that the identities

$$\begin{aligned}&2\int_0^\infty f_0(x)^2 x \,\mathrm{d}x = 1, \\ &2\int_0^\infty f_0(x) f_2(x) x \,\mathrm{d}x = \frac{\pi^2}{6}, \\ &\frac{1}{6}\int_0^\infty (f_0(x) f_4(x) + 3 f_2(x)^2) x \,\mathrm{d}x = \frac{7\pi^4}{360}\end{aligned} \tag{31}$$

are valid numerically with very high degree of accuracy. We have implemented our algorithm for the ε-expansion of sunrise-type diagrams as a simple code in Wolfram's MATHEMATICA system for symbolic manipulations and checked its work-ability and efficiency.

4 Examples

In this section we compute some further examples using our techniques. First we check on a recent result obtained by Laporta for sunrise-type four-loop bubbles [44]. In [44] the difference equation method is used to numerically obtain the coefficients of the Laurent series expansion of all four-loop bubble master integrals. Our results for the sunrise-type topology derived by using configuration space techniques provide an independent check for the results in [44], where momentum space techniques were used to calculate the whole set of four-loop bubble master integrals. This check may help in establishing further confidence in the results of Laporta. As a new application we present the five-loop result for the scalar bubble topology.

4.1 Four-loop vacuum bubble

The four-loop quantity of interest (V_1 in the notation of [44]) is the master integral

$$\tilde{\Pi}_4(p^2=0) = \mathcal{N}_4 \int D(x,m)^5 \mathrm{d}^D x, \tag{32}$$

where the normalization factor $\mathcal{N}_4$ is defined in (10). The Laurent series expansion of the four-loop master integral has been calculated numerically by the difference equation method with high precision in [44]. In Sect. 2 we explained how to obtain the coefficients of its singular part. In fact, we wrote down explicit results for the singular part of the four-loop master integral. In this section we shall compute the finite part and the first three coefficient functions of its ε-expansion numerically using configuration space techniques.

The general idea is really quite straightforward. As explained before, UV divergences reveal themselves in configuration space as singularities of the integrand at small x. We subtract these singularities, obtain a regular integrand, expand the integrand in ε and then finally integrate the integrand numerically [47].

Let us describe our procedure in more detail. We write

$$\begin{aligned}\tilde{\Pi}_4(0) &= \mathcal{N}_4 \int D(x,m)^5 \mathrm{d}^D x \\ &= \mathcal{N}_4 \int D(x,m)(D(x,m)-\Delta(x)+\Delta(x))^4 \mathrm{d}^D x \\ &= \mathcal{N}_4 \int D(x,m) \\ &\quad \times \big((D(x,m)-\Delta(x))^4 + 4(D(x,m)-\Delta(x))^3\Delta(x) \\ &\quad +6\,(D(x,m)-\Delta(x))^2\,\Delta(x)^2 \\ &\quad +4\,(D(x,m)-\Delta(x))\,\Delta(x)^3 + \Delta(x)^4\big)\,\mathrm{d}^D x, \end{aligned} \tag{33}$$

with

$$\Delta(x) = D(x,0) + D_1(x,0) + D_2(x,0), \tag{34}$$

where the functions $D(x,0)$, $D_1(x,0)$, $D_2(x,0)$ subtract singularities of $D(x,m)$ at small x. Their explicit expressions are given in Appendix B. In fact, these functions represent a formal expansion of the massive propagator $D(x,m)$ in the mass parameter m for small m since the real expansion parameter is the dimensionless quantity mx.

One propagator factor $D(x,m)$ in the integrand is left unsubtracted. At large x it provides an IR cutoff. The last two terms of the integrand in (33) can be integrated analytically. They contain all poles in ε and are expressible through Euler's Γ-functions. As expected, the pole part coincides with the expression in (12). Because the analytical expression (as given up to order ε^3 in Appendix C) is rather lengthy, we present only its numerical evaluation,

$$\begin{aligned}&\tilde{\Pi}_4^{\mathrm{ana}}(0) \\ &= m^6\big(-2.5\varepsilon^{-4} - 11.6666667\varepsilon^{-3} - 31.701389\varepsilon^{-2} \\ &\quad -67.528935\varepsilon^{-1} - 15871.965743 - 142923.10240\varepsilon \\ &\quad -701868.64762\varepsilon^2 - 2486982.5547\varepsilon^3 + O(\varepsilon^4)\big). \end{aligned} \tag{35}$$

The first three terms in (33) can be integrated numerically for $D=4$ (i.e. no regularization is necessary) since they are regular at small x. The analytical expression for the functions to be integrated is rather long. The zeroth order ε-coefficient is found in Appendix D (see also the discussion of the integration procedure given in Appendix D). However, as shown in Fig. 3, the functions themselves show a very smooth behavior which renders the numerical integration rather simple. We obtain

$$\begin{aligned}&\tilde{\Pi}_4^{\mathrm{num}}(0) \\ &= m^6\,(15731.745122 + 142349.56687\varepsilon \\ &\quad + 699112.42072\varepsilon^2 + 2468742.6339\varepsilon^3 + O(\varepsilon^4)\big). \end{aligned} \tag{36}$$

The sum of both parts gives

$$\begin{aligned}&\tilde{\Pi}_4(0) \\ &= m^6\big(-2.5\varepsilon^{-4} - 11.6666667\varepsilon^{-3} - 31.701389\varepsilon^{-2} \\ &\quad -67.528935\varepsilon^{-1} - 140.220621 - 573.53553\varepsilon \\ &\quad -2756.22690\varepsilon^2 - 18239.9208\varepsilon^3 + O(\varepsilon^4)\big), \end{aligned} \tag{37}$$

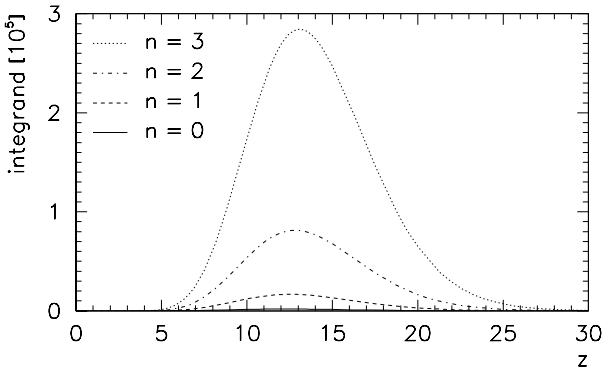

Fig. 3. Integrands for numerical integration in case of the four-loop bubble at different orders in ε

which confirms the known result [44]. The difference to the results of [44] is within the accuracy of the numerical evaluation of the integrals. Therefore, we provide an independent check of this important quantity in full agreement with the results of Laporta.

It is not difficult to extend the analysis to higher orders in ε or to a larger number of significant digits in the coefficients of the ε-expansion. However, since the technique is rather straightforward and simple we do not consider it worthwhile to extend the calculations into these directions. If the need arises, the potential user can tailor and optimize his or her programming code to obtain any desired accuracy and/or order of the ε-expansion. In our evaluation we have used standard tools provided by the MATHEMATICA package which allows reliably control the accuracy of numerical calculations. Even at this early step of improvement it is obvious that our algorithm is extremely simple and efficient.

4.2 Five-loop vacuum bubble

In this subsection we present results for the next order $p^2=0$ sunrise-type diagram, the five-loop vacuum bubble. We have chosen to extend our calculation to the five-loop case since there exist no results on the five-loop bubble in the literature. The integral representation of the five-loop bubble is given by

$$\tilde{\Pi}_5(p^2=0) = \mathcal{N}_5 \int D(x,m)^6 \mathrm{d}^D x. \tag{38}$$

Evaluating numerically the analytical part one obtains

$$\begin{aligned}&\tilde{\Pi}_5^{\mathrm{ana}}(0) \\ &= m^8\big(3\varepsilon^{-5} + 16.5\varepsilon^{-4} + 51.95833\varepsilon^{-3} + 125.6715\varepsilon^{-2} \\ &\quad +259.9876\varepsilon^{-1} - 1360392.5934 - 16888723.177\varepsilon \\ &\quad -111392297.46\varepsilon^2 - 518606741.1\varepsilon^3 + O(\varepsilon^4)\big), \end{aligned} \tag{39}$$

while the numerical integration of the non-singular part gives

$$\tilde{\Pi}_5^{\mathrm{num}}(0)$$

$$= m^8 \left(1360739.9485 + 16886269.683\varepsilon + 111360751.91\varepsilon^2 + 518295438.0\varepsilon^3 + O(\varepsilon^4)\right). \quad (40)$$

The sum of both contributions is given by

$$\begin{aligned}\tilde{\Pi}_5(0) &= m^8 \left(3\varepsilon^{-5} + 16.5\varepsilon^{-4} + 51.95833\varepsilon^{-3} + 125.6715\varepsilon^{-2} \right.\\ &\quad +259.9876\varepsilon^{-1} + 347.3551 - 2453.494\varepsilon\\ &\quad \left. -31545.55\varepsilon^2 - 311303.1\varepsilon^3 + O(\varepsilon^4)\right). \end{aligned} \quad (41)$$

One observes huge cancellation effects between the terms obtained by the analytical calculation and the numerical integration. Apparently the subtraction procedure chosen here is non-optimal. As mentioned before, the subtraction procedure should really be optimized for any given problem in order to avoid a necessity to retain high numerical precision at intermediate steps of calculations. Nevertheless, our non-optimized simple subtraction procedure already works quite reliably with available standard computational tools.

In this section we have described how the configuration space technique works for the case of a trivial numerator. However, our method is applicable and quite efficient also for non-trivial numerator factors as shown in the next section.

5 Irreducible numerator factors in sunrise-type diagrams

For vacuum bubbles of a given topology there can be more than one master integral. For example, in the case of the four-loop sunrise-type bubble topology Laporta identified a second master integral V_2 which has a non-trivial numerator factor which cannot be further reduced [44]. In the momentum representation the non-trivial numerator factors contain scalar products of loop momenta which cannot be further canceled against denominator factors. To be precise, in the case of a n-loop vacuum bubble with $(n+1)$ massive lines, the numerator factor is trivially reducible for $n < 3$. However, starting with $n = 3$ a numerator factor is no longer directly reducible in the general case.

5.1 Three-loop vacuum bubble with irreducible numerator

As an example let us consider the case of a numerator $(k_i \cdot k_j)$ for a vacuum bubble with four massive lines. In momentum space the integral of interest reads

$$\begin{aligned}\tilde{\Pi}_3^*(0) &= \left(\pi^{D/2}\Gamma(3-D/2)\right)^{-3}\\ &\times \int \frac{(k_1\cdot k_3)}{(m_1^2+k_1^2)(m_2^2+(k_2-k_1)^2)}\\ &\quad \times \frac{\mathrm{d}^D k_1 \mathrm{d}^D k_2 \mathrm{d}^D k_3}{(m_3^2+(k_3-k_2)^2)(m_4^2+k_3^2)}. \end{aligned} \quad (42)$$

An expansion of the numerator in terms of invariants,

$$2(k_1\cdot k_3) = k_1^2 + k_3^2 - (k_1-k_3)^2, \quad (43)$$

contains a structure $(k_1-k_3)^2$ which is absent in the denominator. Therefore, the numerator is not directly (trivially) reducible to unity.

In configuration space it is not difficult to treat such a non-trivial numerator since one can reduce the numerator to derivatives of the propagators. The main features of the reduction method are more easily discussed in terms of the equal mass case. The generalization to nonequal mass case is evident. In the above example one can write (using $m_1 = m_2 = \ldots = m$)

$$\tilde{\Pi}_3^*(0) = \mathcal{N}_3 \int D(x,m)^2 \left(\partial_\mu D(x,m)\right)\left(\partial^\mu D(x,m)\right) \mathrm{d}^D x. \quad (44)$$

The integration-by-parts identity takes the form

$$\int \partial_\mu \left(D(x,m)\cdots D(x,m)\right) \mathrm{d}^D x = 0, \quad (45)$$

which, as usual, should be used with the necessary caution.[1] A further useful identity is given by

$$\int \partial^2 \left(D(x,m)\cdots D(x,m)\right) \mathrm{d}^D x = 0. \quad (46)$$

The identities in (45) and (46) lead to a relation between integrals with derivatives. In our example involving four propagators one obtains

$$\begin{aligned}&\int D(x,m)^2 \left(\partial_\mu D(x,m)\left(\partial^\mu D(x,m)\right)\right) \mathrm{d}^D x\\ &\quad = -\frac{1}{3}\int D(x,m)^3 \partial^2 D(x,m) \mathrm{d}^D x. \end{aligned} \quad (47)$$

For the last integral we use $(-\partial^2 + m^2)D(x,m) = \delta(x)$ to end up with

$$\begin{aligned}&\int D(x,m)^3 \partial^2 D(x,m) \mathrm{d}^D x\\ &\quad = m^2 \int D(x,m)^4 \mathrm{d}^D x - D(0,m)^3. \end{aligned} \quad (48)$$

The value of $D(0,m)$ can be found by integration in momentum space,[2]

$$\begin{aligned} D(0,m) &= \frac{1}{(2\pi)^D}\int \frac{\mathrm{d}^D p}{m^2+p^2}\\ &= \frac{2\pi^{D/2}}{(2\pi)^D \Gamma(D/2)} \int_0^\infty \frac{p^{D-1}\mathrm{d}p}{p^2+m^2} \end{aligned}$$

[1] Why this caution is necessary is illustrated by the simple example of a massless propagator. The massless propagator satisfies the equation $-\partial^2 D(x,0) = \delta(x)$, where $\partial^2 = \partial^\mu \partial_\mu$. Integrating the equation over the whole space and dropping the total derivative on the left hand side one obtains the contradiction $0 = 1$ (for details cf. [59]).

[2] $D(0,m)$ can also be obtained by taking the limit $x \to 0$ on the right hand side of (2).

$$= \frac{m^{D-2}}{(4\pi)^{D/2}}\Gamma(1-D/2). \tag{49}$$

Finally we have

$$\tilde{\Pi}_3^*(0) = -\frac{m^2}{3}\tilde{\Pi}_3(0) + \frac{1}{3}\mathcal{N}_3 D(0,m)^3, \tag{50}$$

where $\tilde{\Pi}_3(0)$ is a three-loop sunrise-type bubble diagram without numerators, as calculated earlier. This relation can explicitly be checked.

5.2 Four-loop vacuum bubble with irreducible numerator

As a more realistic example we consider a four-loop diagram that appears as a second independent master integral V_2 of the sunrise topology in the classification of [44]. In momentum space the second master integral V_2 has the additional numerator factor $(k_1 \cdot k_4)^2$ as compared to the first master integral V_1 with unity in the numerator. The second master integral reads

$$\tilde{\Pi}_4^*(0) = \left(\pi^{D/2}\Gamma(3-D/2)\right)^{-4} \times \int \frac{(k_1\cdot k_4)^2}{(m_1^2+k_1^2)(m_2^2+(k_2-k_1)^2)(m_3^2+(k_3-k_2)^2)} \times \frac{\mathrm{d}^D k_1 \mathrm{d}^D k_2 \mathrm{d}^D k_3 \mathrm{d}^D k_4}{(m_4^2+(k_4-k_3)^2)(m_5^2+k_4^2)}. \tag{51}$$

Turning again to the equal mass case and using the configuration space representation, this integral can be written as

$$\tilde{\Pi}_4^*(0) = \mathcal{N}_4 \int D(x,m)^3 (\partial_\mu\partial_\nu D(x,m))(\partial_\mu\partial_\nu D(x,m))\mathrm{d}^D x. \tag{52}$$

It is apparent that by using integration-by-parts techniques this integral cannot be reduced to scalar integrals and/or integrals containing d'Alembertians. The easiest way to evaluate such an integral is to compute the derivatives directly. This is done by using

$$\frac{1}{z}\frac{\mathrm{d}}{\mathrm{d}z}\left(z^{-\nu}K_\nu(z)\right) = -\left(z^{-\nu-1}K_{\nu+1}(z)\right). \tag{53}$$

This relation can be iterated and gives results for arbitrary high order derivatives of Bessel functions $K_\lambda(z)$ in terms of the same class of Bessel functions with shifted indices and powers in z. For the first derivative we obtain

$$\partial_\mu D(x,m) = -x_\mu \frac{m^{2\lambda+2}}{(2\pi)^{\lambda+1}}\frac{K_{\lambda+1}(mx)}{(mx)^{\lambda+1}}. \tag{54}$$

Since the resulting analytical expression for the given line of the diagram lies in the same class as the original line, the procedure of evaluation of the integral is similar to the usual one. However, we cannot use the second derivative

$$\partial_\mu\partial_\nu D(x,m) = \frac{m^{2\lambda+2}}{(2\pi)^{\lambda+1}(mx)^{\lambda+1}} \times \left(g_{\mu\nu}K_{\lambda+2}(mx) - \frac{x_\mu x_\nu}{x^2}K_{\lambda+1}(mx)\right) \tag{55}$$

directly under the integration sign. The reason is that if the propagator is considered as a distribution, there is a δ-function singularity at the origin which is not taken into account in (55). Indeed, contracting the indices μ an ν in (55) one obtains

$$\partial_\mu\partial_\mu D(x,m) = m^2 D(x,m), \tag{56}$$

while the correct equation for the propagator reads $(-\partial^2 + m^2)D(x,m) = \delta(x)$. Thus, the straightforward evaluation of derivatives is always valid only for $x = 0$. The behavior at the origin ($x = 0$) requires a special consideration. In practice, to treat this situation one should not use higher order derivatives but stay at the level of first derivatives.

In order to deal with this situation we introduce another master integral

$$\tilde{\Pi}_4^{**}(0) = \mathcal{N}_4 \int D(x,m)\partial_\mu D(x,m)\partial_\nu D(x,m) \times \partial^\mu D(x,m)\partial^\nu D(x,m)\mathrm{d}^D x. \tag{57}$$

The relation between the two master integrals $\Pi_4^*(0)$ and $\Pi_4^{**}(0)$ is found to be

$$\tilde{\Pi}_4^*(0) = 3\tilde{\Pi}_4^{**}(0) - \frac{1}{8}m^4\tilde{\Pi}_4(0) - \frac{7}{8}m^2\mathcal{N}_4 D(0,m)^4. \tag{58}$$

The quantity $\tilde{\Pi}_4^{**}(0)$ can be calculated with the explicit use of first order derivatives within our technique. We obtain the analytical result for the pole part

$$\tilde{\Pi}_4^{**}(0)m^{10} \times \left(-\frac{3}{8\varepsilon^4} - \frac{277}{144\varepsilon^3} - \frac{37837}{6912\varepsilon^2} - \frac{4936643}{414720\varepsilon} + O(\varepsilon^0)\right) \tag{59}$$

and the ε-expansion in the form

$$\tilde{\Pi}_4^{**}(0) = m^{10}\left(-0.375\varepsilon^{-4} - 1.923611\varepsilon^{-3} - 5.474103\varepsilon^{-2} - 11.90356\varepsilon^{-1} - 27.99303 - 104.5384\varepsilon - 663.6123\varepsilon^2 - 3703.241\varepsilon^3 + O(\varepsilon^4)\right). \tag{60}$$

Since the results for $\tilde{\Pi}_4(0)$, $\tilde{\Pi}_4^{**}(0)$, and $D(0,m)^4$ are known, (58) can be used to obtain the final result for the original integral,

$$\tilde{\Pi}_4^*(0) = m^{10}\left(-1.6875\varepsilon^{-4} - 7.8125\varepsilon^{-3} - 21.20964\varepsilon^{-2} - 44.76955\varepsilon^{-1} - 97.07652 - 290.9234\varepsilon - 1719.809\varepsilon^2 - 8934.731\varepsilon^3 + O(\varepsilon^4)\right), \quad (61)$$

which again verifies the result given in [44].

Differentiation of the massive propagator leads to expressions of a similar functional form which makes the configuration space technique a universal tool for calculating any master integral of the sunrise topology. This technique is also useful for finding master integrals. Indeed, new master integrals appear when there is a possibility to add new derivatives into integrands which cannot be eventually removed by using the equations of motion or integration-by-parts recurrence relations. But once again: without explicit inclusion of the δ-function only one derivative is allowed. Otherwise one runs into problems not seeing some parts (tadpoles) of the result. Therefore, the new master integral should contain just one derivative for each line excepting one line. For instance, in the five-loop case (six propagators) there will be only two master integrals.

6 Summary and conclusions

We have suggested a new efficient technique to compute diagrams of the sunrise-type topology with any number of loops at any order of the ε-expansion for any mass configuration. For a given number of loops the sunset-type topology constitutes only a small fraction of the whole set of multi-loop topologies that need to be calculated. Nevertheless, our results on the subset of sunrise-type diagrams provide a necessary check on multi-loop results calculated by other techniques and therefore can be very useful for many multi-loop calculations. We have also worked out a few examples with non-trivial numerator factors. Valuable by itself, our method can be used to check the results of other techniques.

Acknowledgements. We thank K.G. Chetyrkin for his constructive, yet exacting criticism in the course of our work on the application of x-space techniques to the evaluation of sunrise diagrams. We thank R. Delbourgo for his kind attention and enthusiasm in advertising and developing x-space techniques and G. Passarino for a communication. We would also like to thank J. Gasser for his interest and discussions. AAP thanks V.A. Matveev for encouragement, attention and support. This work is partially supported by the Volkswagen grant I/77 788, the RFBR grants # 02-01-00601 and # 03-02-17177, and the Estonian target financed project No. 0182647s04. S. Groote acknowledges support from a grant given by the Graduiertenkolleg "Eichtheorien", Mainz University.

A Singular contributions for arbitrary masses

In the following we present complete results for the singular parts of sunrise-type diagrams with arbitrary masses up to four-loop order. The results are given in the $\overline{\rm MS}$-scheme in the Euclidean domain. We have

$$\tilde{\Pi}_1^s(p,m_1,m_2) = \frac{1}{\varepsilon},$$

$$\tilde{\Pi}_2^s(p,m_1,m_2,m_3) = -\frac{1}{2\varepsilon^2}\sum_i m_i^2 - \frac{1}{4\varepsilon}\left(p^2 + 2\sum_i m_i^2(3-2\ell_i)\right),$$

$$\tilde{\Pi}_3^s(p,m_1,m_2,m_3,m_4) = \frac{1}{6\varepsilon^3}\sum_{i\neq j} m_i^2 m_j^2 + \frac{1}{12\varepsilon^2}\left(p^2\sum_i m_i^2 - \sum_i m_i^4 + 2\sum_{i\neq j} m_i^2 m_j^2\,(4-3\ell_i)\right) + \frac{1}{72\varepsilon}\left(2p^4 + 9p^2\sum_i m_i^2(3-2\ell_i) - 9\sum_i m_i^4(5-2\ell_i) + 6\sum_{i\neq j} m_i^2 m_j^2(20-24\ell_i+3\ell_i^2+6\ell_i\ell_j)\right),$$

$$\tilde{\Pi}_4^s(p,m_1,m_2,m_3,m_4,m_5) = -\frac{1}{24\varepsilon^4}\sum_{i\neq j\neq k} m_i^2 m_j^2 m_k^2 - \frac{1}{48\varepsilon^3}\left(p^2\sum_{i\neq j} m_i^2 m_j^2 - \sum_{i\neq j}(m_i^4 m_j^2 + m_i^2 m_j^4) + 2\sum_{i\neq j\neq k} m_i^2 m_j^2 m_k^2(5-4\ell_i)\right) - \frac{1}{288\varepsilon^2}\left(2p^4\sum_i m_i^2 - 6p^2\sum_i m_i^4 + 2\sum_i m_i^6 + 3p^2\sum_{i\neq j} m_i^2 m_j^2(11-8\ell_i) - 6\sum_{i\neq j}(m_i^4 m_j^2 + m_i^2 m_j^4)(7-4\ell_i) + 12\sum_{i\neq j\neq k} m_i^2 m_j^2 m_k^2(15-20\ell_i+2\ell_i^2+6\ell_i\ell_j)\right) - \frac{1}{1728\varepsilon}\left(3p^6 + 2p^4\sum_i m_i^2(35-24\ell_i) - 18p^2\sum_i m_i^4(21-8\ell_i) + 2\sum_i m_i^6(77-24\ell_i) + 9p^2\sum_{i\neq j} m_i^2 m_j^2(71-88\ell_i+8\ell_i^2+24\ell_i\ell_j) - 216\sum_{i\neq j}(m_i^4 m_j^2 - m_i^2 m_j^4)\ell_i - 18\sum_{i\neq j}(m_i^4 m_j^2 + m_i^2 m_j^4)(49-56\ell_i+4\ell_i^2+12\ell_i\ell_j) + 24\sum_{i\neq j\neq k} m_i^2 m_j^2 m_k^2(105-180\ell_i+30\ell_i^2$$

$$+90\ell_i\ell_j - 2\ell_i^3 - 18\ell_i^2\ell_j - 12\ell_i\ell_j\ell_k)\big)\,, \tag{62}$$

where $\ell_i = \ln(m_i^2/\mu^2)$. The indices i, j, and k run over all mass indices. One can check that the general results listed in this appendix reproduce the equal mass results listed in the main text.

B Explicit form of subtraction terms for the small x singularities

The leading singularity at small x is given by the massless propagator of the form

$$D(x,0) = \frac{\Gamma(\lambda)}{4\pi^{\lambda+1}x^{2\lambda}}. \tag{63}$$

The next order of the small x-expansion for the propagator $D(x,m)$ is explicitly given by

$$D_1(x,0) = \frac{1}{4\pi^{\lambda+1}x^{2\lambda}} \times \left(\left(\frac{x}{2}\right)^2 \frac{\Gamma(\lambda)}{1-\lambda} - \left(\frac{x}{2}\right)^{2\lambda} \frac{\Gamma(1-\lambda)}{\lambda}\right). \tag{64}$$

This term is suppressed relative to the first term by one power of x^2 at small x in four-dimensional space-time (however, this is not the case for two-dimensional space-time with $\lambda = 0$). The term

$$D_2(x,0) = \frac{1}{4\pi^{\lambda+1}x^{2\lambda}} \left(\frac{x}{2}\right)^2 \times \left(\left(\frac{x}{2}\right)^2 \frac{\Gamma(\lambda)}{2(1-\lambda)(2-\lambda)} - \left(\frac{x}{2}\right)^{2\lambda} \frac{\Gamma(1-\lambda)}{\lambda(\lambda+1)}\right) \tag{65}$$

is further suppressed by one power of x^2 at small x. Therefore, the full subtraction of the three terms gives a rather smooth behavior at small x which is sufficient to obtain a regular integrand for the numerical integration.

C Analytical results for the four-loop sunrise diagram

In this appendix we present some more details of our calculations for the four-loop sunrise diagram. For the analytical evaluation we take the last two terms of the integrand from (33). One has to integrate a product of two Bessel functions with powers of x which can be done analytically. The explicit expression for the ε-expansion of that part of the integral which is evaluated analytically reads

$$\begin{aligned}
&\tilde{\Pi}_4^{\rm ana}(0) \\
&= m^6 \Bigg\{ -\frac{5}{2\varepsilon^4} - \frac{35}{3\varepsilon^3} - \frac{4565}{144\varepsilon^2} - \frac{58345}{864\varepsilon} \\
&\quad - \frac{1456940638037}{7779240000} - \frac{17099\pi^2}{24} - \frac{3857\pi^4}{10} \\
&\quad + \frac{2525968\zeta(3)}{105} \\
&\quad + \Bigg(-\frac{55171475321621447}{1633640400000} + \frac{2457509\pi^2}{144} \\
&\quad - \frac{1292537\pi^4}{175} + \frac{6752474831\zeta(3)}{44100} \\
&\quad + 16530\pi^2\zeta(3) + 59508\zeta(5) \Big)\varepsilon \\
&\quad + \Bigg(-\frac{10610679621089130529}{68612896800000} + \frac{92781949\pi^2}{864} \\
&\quad - \frac{4290113759\pi^4}{110250} - \frac{22591\pi^6}{14} \\
&\quad + \frac{952412727629\zeta(3)}{9261000} + 244476\pi^2\zeta(3) \\
&\quad - 168606\zeta(3)^2 + \frac{32210272\zeta(5)}{35} \Bigg)\varepsilon^2 \\
&\quad + \Bigg(-\frac{5963907632629558995931}{14408708328000000} + \frac{1325204033\pi^2}{5184} \\
&\quad - \frac{464379085699\pi^4}{6615000} - \frac{48529231\pi^6}{2205} \\
&\quad - \frac{312138383154103\zeta(3)}{277830000} + \frac{7285043\pi^2\zeta(3)}{6} \\
&\quad + 43529\pi^4\zeta(3) - \frac{238229084\zeta(3)^2}{105} \\
&\quad + \frac{13583011297\zeta(5)}{2940} + 247950\pi^2\zeta(5) \\
&\quad + 1190160\zeta(7) \Big)\varepsilon^3 + O(\varepsilon)^4 \Big\}\,.
\end{aligned} \tag{66}$$

This expression shows the real complexity of the calculation which reveals itself in the structure of the results. The main feature is that the terms cannot be simultaneously simplified to all orders in ε. By a special choice of the normalization factor one can make the leading term and, in fact, even all pole terms simple, but then the higher order terms contain rather lengthy combinations of transcendental numbers that are not reducible in terms of standard quantities such as the Riemann ζ-functions. Note also that the rational coefficients of transcendental numbers are very big and there is a huge numerical cancellation between the rational and transcendental parts of the answer (see also the discussion in [56]).

D Integrand for numerical integration

For the numerical evaluation we take the first three terms of the integrand from (33). One has to integrate them numerically as there is a product of three or more Bessel functions which is too complicated to be done analytically. To find the ε-expansion of the integral one has to first expand the integrand in ε. The expression for the ε-expansion is quite lengthy. We therefore give explicit results only for $\varepsilon = 0$. For this part the integrand for the numerical integration over $z = mx$ reads

$$\begin{aligned}
&\Pi_4^{\rm num}(x) \\
&= m^6 \Bigg(66 - 108l - 144l^2 + 192l^3 + \frac{384}{z^6} - \frac{384}{z^4} + \frac{768l}{z^4}
\end{aligned}$$

$$
\begin{aligned}
&+\frac{24}{z^2}-\frac{480l}{z^2}+\frac{576l^2}{z^2}-\frac{111z^2}{16}+\frac{147lz^2}{2}-117l^2z^2\\
&+24l^3z^2+24l^4z^2+-\frac{165z^4}{32}+\frac{201lz^4}{16}+\frac{9l^2z^4}{2}\\
&-24l^3z^4+12l^4z^4+\frac{75z^6}{512}-\frac{405lz^6}{128}+\frac{531l^2z^6}{64}\\
&-\frac{15l^3z^6}{2}+\frac{9l^4z^6}{4}+\frac{375z^8}{2048}-\frac{825lz^8}{1024}+\frac{315l^2z^8}{256}\\
&-\frac{51l^3z^8}{64}+\frac{3l^4z^8}{16}+\frac{1875z^{10}}{131072}-\frac{375lz^{10}}{8192}+\frac{225l^2z^{10}}{4096}\\
&-\frac{15l^3z^{10}}{512}+\frac{3l^4z^{10}}{512}\Bigg)K_1(z)\\
&+m^6\left(\frac{-512}{z^5}+\frac{384}{z^3}-\frac{768l}{z^3}+\frac{24}{z}+\frac{288l}{z}-\frac{384l^2}{z}\right.\\
&-52z+120lz-64l^3z-\frac{15z^3}{8}-21lz^3+48l^2z^3\\
&-24l^3z^3+\frac{75z^5}{32}-\frac{135lz^5}{16}+9l^2z^5-3l^3z^5\\
&\left.+\frac{125z^7}{512}-\frac{75lz^7}{128}+\frac{15l^2z^7}{32}-\frac{l^3z^7}{8}\right)K_1(z)^2\\
&+m^6\frac{128K_1(z)^5}{z^2}. \qquad (67)
\end{aligned}
$$

Here $l=\ln(\mathrm{e}^\gamma z/2)$, $z=mx$, and $\gamma=-\Gamma'(1)$ is Euler's constant. As shown in Fig. 3, the plot of this function as well as the shapes of the corresponding functions in higher orders of ε are very smooth and quite similar. The analytical expressions for higher orders in ε, however, become much longer. Note that the new functions $f_n(z)$ first appear at order ε^2.

The smoothness of the zeroth order integrand as shown in (67) implies that the numerical integration is quite easy to execute. Because the integrand vanishes exponentially for large values of z and has no singularities of the kind $z\ln z$ for small values of z, the integration can in principle range from 0 to ∞. However, for practical reasons we had to instruct MATHEMATICA (which we used for all of our calculations presented here) that the integrand vanishes for $z=0$. On the other hand, the asymptotic expansion of the integrand together with the integration measure is dominated by the term

$$
\frac{6\pi^2m^2}{512}z^{10}\ln^4(\mathrm{e}^\gamma z/2)K_1(z)z^3 \qquad \left(K_\lambda(z)\to\sqrt{\frac{\pi}{2z}}\mathrm{e}^{-z}\text{ for }z\to\infty\right). \qquad (68)
$$

Integrated over z from Λ to ∞, this part gives a contribution

$$
\frac{6\pi^2m^2}{512}\Lambda^{25/2}\ln^4(\mathrm{e}^\gamma\Lambda/2)\mathrm{e}^{-\Lambda} \qquad (69)
$$

and terms which are of subleading order. Therefore, the result can be well estimated by

$$
\begin{aligned}
\tilde{\Pi}_4^{\mathrm{num}}(0)&=2\pi^2\int_0^\infty \Pi_4^{\mathrm{num}}(x)x^3\mathrm{d}x\\
&\approx 2\pi^2\int_0^\Lambda \Pi_4^{\mathrm{num}}(x)x^3\mathrm{d}x\\
&\quad+\frac{6\pi^2m^2}{512}\Lambda^{25/2}\ln^4(\mathrm{e}^\gamma\Lambda/2)\mathrm{e}^{-\Lambda} \qquad (70)
\end{aligned}
$$

and Λ can be adjusted in such a way that any desired precision is obtained.

A possibility to avoid any kind of cutoff is to change the integration variable in the sense that the interval $[0,\infty]$ is mapped onto $[0,1]$. Then the integration can be done numerically with the additional information that the integrand vanishes identically at both end points. Possible transformations of this kind are for instance $z=\ln(1/t)$ or $z=(1-t)/t$ for $t\in[0,1]$.

References

1. P. Langacker (ed.), Precision Tests of the Standard Electroweak Model (World Scientific, 1995)
2. W. Hollik, The electroweak Standard Model, prepared for the ICTP Summer School in Particle Physics, Trieste, Italy, 21 June–9 July 1999
3. J. Blümlein, F. Jegerlehner, T. Riemann, W. Hollik, J.H. Kühn, Application Of Quantum Field Theory To Phenomenology – Loops And Legs In Quantum Field Theory, Proceedings of the 6th International Symposium, Radcor 2002, and the 6th Zeuthen Workshop, Kloster Banz, Germany, September 8–13, 2002
4. J.G. Körner, A.I. Onishchenko, A.A. Petrov, A.A. Pivovarov, Phys. Rev. Lett. **91**, 192002 (2003); J.H. Kühn, A.I. Onishchenko, A.A. Pivovarov, O.L. Veretin, Phys. Rev. D **68**, 033018 (2003); S. Groote, J.G. Körner, A.A. Pivovarov, Eur. Phys. J. C **24**, 393 (2002)
5. K.G. Chetyrkin, F.V. Tkachov, Nucl. Phys. B **192**, 159 (1981); F.V. Tkachov, Phys. Lett. B **100**, 65 (1981)
6. D.J. Broadhurst, Z. Phys. C **54**, 599 (1992)
7. P.A. Baikov, Phys. Lett. B **385**, 404 (1996)
8. K.G. Chetyrkin, J.H. Kühn, M. Steinhauser, Nucl. Phys. B **482**, 213 (1996)
9. S. Laporta, E. Remiddi, Phys. Lett. B **379**, 283 (1996)
10. O.V. Tarasov, Nucl. Phys. B **502**, 455 (1997)
11. T. Gehrmann, E. Remiddi, Nucl. Phys. B **580**, 485 (2000)
12. K. Melnikov, T. van Ritbergen, Nucl. Phys. B **591**, 515 (2000)
13. S. Laporta, Int. J. Mod. Phys. A **15**, 5087 (2000)
14. A.G. Grozin, Nucl. Instrum. Meth. A **502**, 610 (2003)
15. C.S. Meijer, Proc. Amsterdam Akad. Wet. **599**, 702 (1940)
16. B. Almgren, Arkiv för Fysik **38**, 161 (1967); S. Bauberger, F.A. Berends, M. Böhm, M. Buza, Nucl. Phys. B **434**, 383 (1995)
17. E. Mendels, Nuovo Cim. A **45**, 87 (1978)
18. L.V. Avdeev, Comput. Phys. Commun. **98**, 15 (1996)
19. S. Groote, J.G. Körner, A.A. Pivovarov, Phys. Rev. D **60**, 061701 (1999)
20. Y. Schröder, Nucl. Phys. Proc. Suppl. **116**, 402 (2003)
21. S.A. Larin, V.A. Matveev, A.A. Ovchinnikov, A.A. Pivovarov, Yad. Fiz. **44**, 1066 (1986); I.I. Balitsky, D. Diakonov, A.V. Yung, Phys. Lett. B **112**, 71 (1982); K.G. Chetyrkin, S. Narison, Phys. Lett. B **485**, 145 (2000); H.Y. Jin, J.G. Körner, T.G. Steele, Phys. Rev. D **67**, 014025 (2003)

22. T. Sakai, K. Shimizu, K. Yazaki, Prog. Theor. Phys. Suppl. **137**, 121 (2000)
23. S. Groote, A.A. Pivovarov, Eur. Phys. J. C **21**, 133 (2001); JETP Lett. **75**, 221 (2002)
24. A.A. Ovchinnikov, A.A. Pivovarov, L.R. Surguladze, Sov. J. Nucl. Phys. **48**, 358 (1988); Int. J. Mod. Phys. A **6**, 2025 (1991); S. Groote, J.G. Körner, A.A. Pivovarov, Phys. Rev. D **61**, 071501 (2000); Analytical calculation of heavy baryon correlators in NLO of perturbative QCD, in Batavia 2000, Advanced computing and analysis technique in physics research 277–279 [hep-ph/0009218]
25. S. Narison, A.A. Pivovarov, Phys. Lett. B **327**, 341 (1994)
26. S.R. Coleman, E. Weinberg, Phys. Rev. D **7**, 1888 (1973); R. Jackiw, Phys. Rev. D **9**, 1686 (1974); R. Jackiw, S. Templeton, Phys. Rev. D **23**, 2291 (1981); J.M. Chung, B.K. Chung, J. Korean Phys. Soc. **39**, 971 (2001); Phys. Rev. D **59**, 105014 (1999)
27. D.J. Gross, R.D. Pisarski, L.G. Yaffe, Rev. Mod. Phys. **53**, 43 (1981); T. Appelquist, R.D. Pisarski, Phys. Rev. D **23**, 2305 (1981); T. Hatsuda, Nucl. Phys. A **544**, 27 (1992)
28. J.O. Andersen, E. Braaten, M. Strickland, Phys. Rev. D **62**, 045004 (2000)
29. T. Nishikawa, O. Morimatsu, Y. Hidaka, Phys. Rev. D **68**, 076002 (2003)
30. A.K. Rajantie, Nucl. Phys. B **480**, 729 (1996) [Erratum B **513**, 761 (1998)]
31. L. Platter, H.W. Hammer, U.G. Meissner, Nucl. Phys. A **714**, 250 (2003); J.F. Yang, J. Zhou, C. Wu, Commun. Theor. Phys. **40**, 461 (2003); H. Van Hees, J. Knoll, Phys. Rev. D **65**, 105005 (2002); C. Felline, N.P. Mehta, J. Piekarewicz, J.R. Shepard, Phys. Rev. C **68**, 034003 (2003)
32. E. Witten, Nucl. Phys. B **160**, 57 (1979)
33. K. Kajantie, M. Laine, K. Rummukainen, Y. Schröder, JHEP **0304**, 036 (2003)
34. P. Post, K. Schilcher, Phys. Rev. Lett. **79**, 4088 (1997)
35. P. Post, J.B. Tausk, Mod. Phys. Lett. A **11**, 2115 (1996)
36. J. Gasser, M.E. Sainio, Eur. Phys. J. C **6**, 297 (1999)
37. R. Delbourgo, M.L. Roberts, J. Phys. A **36**, 1719 (2003)
38. A. Bashir, R. Delbourgo, M.L. Roberts, J. Math. Phys. **42**, 5553 (2001)
39. N.E. Ligterink, Phys. Rev. D **61**, 105010 (2000); B. Kastening, H. Kleinert, Phys. Lett. A **269**, 50 (2000)
40. A.I. Davydychev, V.A. Smirnov, Nucl. Phys. B **554**, 391 (1999)
41. E. Mendels, J. Math. Phys. **43**, 3011 (2002)
42. M. Caffo, H. Czyż, E. Remiddi, Nucl. Phys. B **634**, 309 (2002); Nucl. Phys. Proc. Suppl. **116**, 422 (2003)
43. I. Bierenbaum, S. Weinzierl, Eur. Phys. J. C **32**, 67 (2003)
44. S. Laporta, Phys. Lett. B **549**, 115 (2002)
45. G. Passarino, Nucl. Phys. B **619**, 257 (2001)
46. S. Groote, J.G. Körner, A.A. Pivovarov, Phys. Lett. B **443**, 269 (1998)
47. S. Groote, J.G. Körner, A.A. Pivovarov, Nucl. Phys. B **542**, 515 (1999)
48. S. Groote, A.A. Pivovarov, Nucl. Phys. B **580**, 459 (2000)
49. G.N. Watson, Theory of Bessel functions (Cambridge, 1944)
50. K.G. Chetyrkin, A.L. Kataev, F.V. Tkachov, Nucl. Phys. B **174**, 345 (1980)
51. A.E. Terrano, Phys. Lett. B **93**, 424 (1980)
52. N.N. Bogoliubov, D.V. Shirkov, Quantum fields (Benjamin, 1983)
53. A.P. Prudnikov, Yu.A. Brychkov, O.I. Marichev, Integrals and Series, Vol. 2 (Gordon and Breach, New York 1990)
54. I.S. Gradshteyn, I.M. Ryzhik, Tables of integrals, series, and products (Academic Press, 1994)
55. E. Braaten, A. Nieto, Phys. Rev. D **51**, 6990 (1995)
56. S. Groote, J.G. Körner, A.A. Pivovarov, Eur. Phys. J. C **11**, 279 (1999)
57. A.I. Davydychev, M.Y. Kalmykov, Nucl. Phys. B **605**, 266 (2001)
58. A.T. Suzuki, A.G.M. Schmidt, ε-expansion for non-planar double-boxes, hep-ph/0401207
59. A.P. Isaev, Nucl. Phys. B **662**, 461 (2003); S.G. Gorishnii, A.P. Isaev, Theor. Math. Phys. **62**, 232 (1985) [Teor. Mat. Fiz. **62**, 345 (1985)]